Design and Implementation of an Output Regulation Controller for the JET Tokamak

Giuseppe Ambrosino, Marco Ariola, *Senior Member, IEEE*, Alfredo Pironti, and Filippo Sartori

***Abstract*—This paper describes the design and the experimental validation of a multivariable current and shape controller for the Joint European Torus (JET) tokamak. Using this new controller, physicists have been able to carry out experiments where accurate control of the plasma boundary is needed. From a control point of view, the problem has been formulated as an output regulation problem for a linear time-invariant (LTI) plant whose controllable outputs are more than the control inputs. For the case of constant references, we propose a control scheme that minimizes a quadratic cost function. This cost function weights the tracking error at steady state. Our methodology is based on the singular value decomposition of the static gain matrix of the plant. In the controller design, we can also take into account the steady-state control effort. The proposed controller has been implemented and tested on the plant; some experimental results are included in this paper. The activity that has been carried out and that is described in this paper is relevant in the perspective of the new experimental reactor ITER.**

***Index Terms*—Experimental results, nuclear fusion, output regulation, plasma control, power plants.**

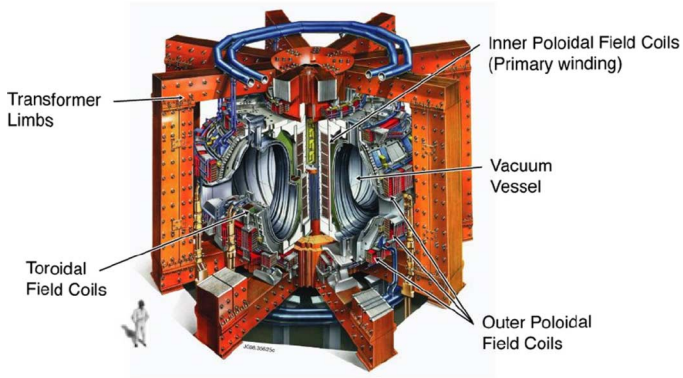

Fig. 1. Schematic drawing of the coil system in the JET tokamak. The electromagnetic fields that control plasma shape, position, and current, are generated by the currents flowing in a set of poloidal field coils distributed around the vacuum vessel. These currents are driven in feedback on the basis of measurements of the plasma position and boundary (courtesy of EFDA-JET).

I. Introduction

THE RAPID consumption of fossil fuels pushes toward the search of new resources. Fusion reactions power the sun and other stars. In fusion reactions, low-mass nuclei combine, or fuse, to form more massive nuclei. The fusion process converts mass into kinetic energy. The principal nuclear reactions are those involving light nuclei, such as the hydrogen isotope deuterium; deuterium can easily and cheaply be extracted from water and the amount of deuterium in the oceans is essentially unlimited. Therefore, in principle, the fuel sources are essentially inexhaustible; moreover, the fusion process is inherently safe and a limited amount of harmful by-products are produced.

For nuclear fusion to happen, it is necessary to heat the fuel to a sufficiently high temperature at which the thermal velocities of the nuclei are high enough to produce the desired reactions. The necessary temperature is around 100 million degrees Celsius. At such temperature an important fraction of the gas is *ionized*, so that the electrons and ions are separately free. This gas, which can be shown to be quasi-neutral, is called *plasma*. One possible approach for nuclear fusion on earth is the magnetic confinement of a plasma in suitable devices. Among the various possible configurations, the most promising approach has proved to be the *tokamak*.

The term "tokamak" comes from the Russian words **to**roidalnaya **ka**mera and **ma**nitnaya **k**atushka, which mean "toroidal chamber" and "magnetic coil." As indicated by the name, tokamaks are magnetic confinement devices constructed in the shape of a torus (or doughnut). This device was invented in the Soviet Union with the early developments taking place in the late 1950s. In a schematic description (see Fig. 1 for the case of the JET tokamak), the tokamak is composed of: 1) a vessel where the plasma is confined (*vacuum vessel*); 2) some poloidal coils that are used to produce the toroidal field (*toroidal field coils*); and 3) other coils that are needed to generate the poloidal field (*poloidal field coils*).

The confinement of the plasma is obtained via the interaction of the plasma with an external electromagnetic field, produced by the toroidal coils. High performance in tokamaks are achieved by plasmas with elongated poloidal cross-section; this elongation causes the plasma vertical position to be unstable. Therefore, the use of feedback for position control is mandatory. Moreover, to use in the best possible way the available chamber volume, the plasma needs to be placed as close as possible to the plasma facing components. Although the plasma facing components are designed to withstand high heat fluxes, contact with

Manuscript received May 19, 2006; revised May 8, 2007. Manuscript received in final form December 10, 2007. First published June 10, 2008; current version published October 22, 2008. Recommended by Associate Editor D. Rivera. This work was supported in part by EURATOM under the European Fusion Development Agreement.

G. Ambrosino and A. Pironti are with the Associazione Euratom/ENEA/CREATE, Dipartimento di Informatica e Sistemistica, Università degli Studi di Napoli Federico II, 80125 Napoli, Italy (e-mail: ambrosin@unina.it; pironti@unina.it).

M. Ariola is with the Associazione Euratom/ENEA/CREATE, Dipartimento per le Tecnologie, Università degli Studi di Napoli Parthenope, Centro Direzionale di Napoli, 80143 Napoli, Italy (e-mail: ariola@uniparthenope.it).

F. Sartori is with Euratom/UKAEA Fusion Association, Culham Science Centre, Abingdon, Oxon OX14 3DB, U.K. (e-mail: filippo.sartori@jet.uk).

Color versions of one or more of the figures in this paper are available online at http://ieeexplore.ieee.org.

Digital Object Identifier 10.1109/TCST.2008.917216

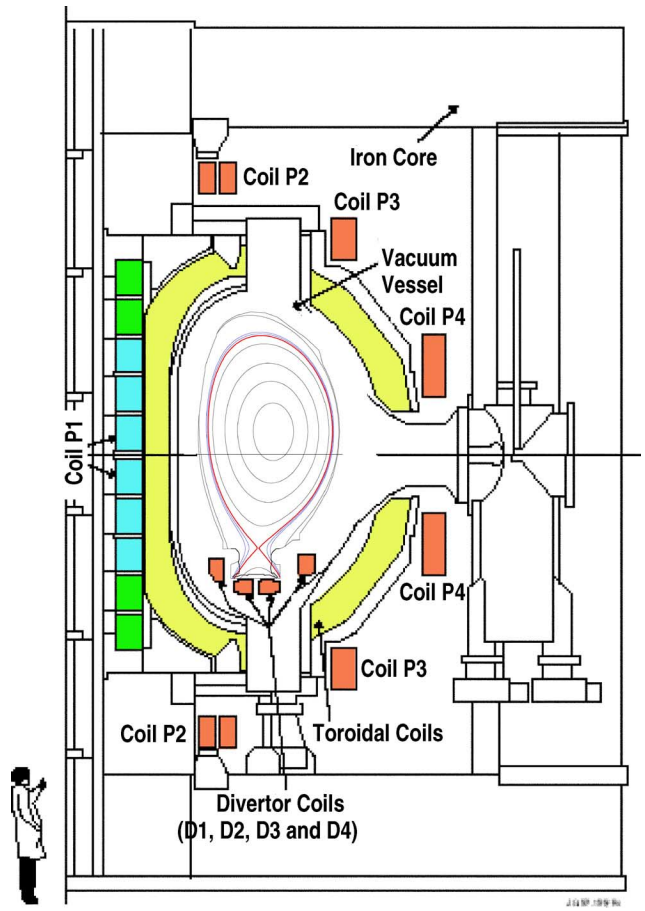

Fig. 2. JET cross section. The plasma boundary is shown in red. The poloidal coils (P1–P4 and D1–D4) and the toroidal coils, which surround the plasma ring, produce the necessary confinement magnetic field (courtesy of EFDA-JET).

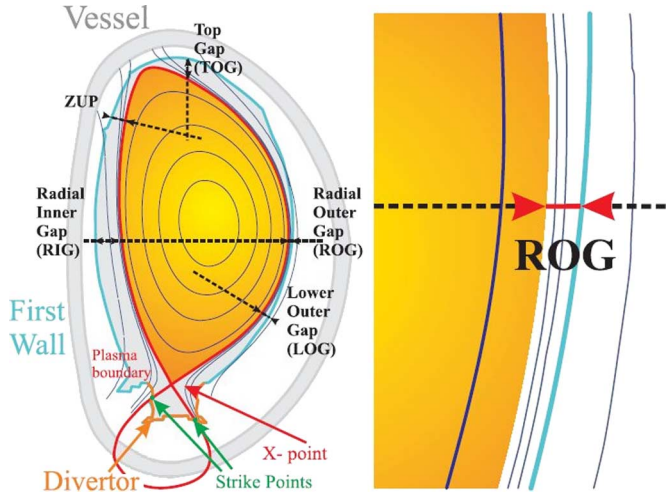

Fig. 3. On the left, the figure shows some of the plasma-wall distances, called *gaps*, defined for the JET control system. Note that a gap is not strictly the distance between the plasma surface and a wall point, but rather the distance measured on a certain line. The figure also shows the divertor region, with the X-point and the strike points. On the right, a close-up of the ROG gap.

the plasma is always a major concern in tokamak operations and, therefore, adequate plasma-wall clearance must be guaranteed. This is obtained by means of additional magnetic fields produced by suitable currents flowing in a number of poloidal field coils surrounding the plasma ring. These currents are generated by a power supply system driven in feedback by a plasma shape control system. Fig. 2 shows the poloidal field coils of the Joint European Torus (JET) tokamak.

In the first experiments on tokamaks with elongated plasmas, feedback control was used only to stabilize the unstable mode. Successively, other geometrical parameters were controlled in feedback. The control of few geometrical parameters is no longer sufficient when the plasma shape has to be guaranteed with very high accuracy. In these cases, usually the controlled shape geometrical descriptors are the distances between the plasma boundary and the vessel at some specific points. These plasma-wall distances are called *gaps*; some gaps defined for the JET control system are shown in Fig. 3. In the next generation tokamak, the plasma-wall distance must be carefully controlled during the main part of the experiment with a degree of accuracy of a few centimeters. When high performance is required, the strong output coupling calls for a model-based multiple-input–multiple-output (MIMO) approach to obtain adequate closed-loop performance.

Model-based control design approaches have been used recently to control the plasma vertical position in [1], where the authors use the H_∞ technique; in [2], where predictive control is adopted; in [3], where a nonlinear, adaptive controller is designed; in [4], where an anti-windup synthesis is proposed to allow operation of the vertical controller in the presence of saturation; in [5], where a fuzzy-logic-based controller is designed and implemented to control the position of the plasma column throughout an entire discharge.

There are few examples of multivariable controllers used for position, current, and shape control. In [6] normalized coprime factorization is used to control the shape of the DIII-D plasma. In [7] and [8] the authors propose a controller designed using the H_∞ technique, which has been used during normal tokamak operation to control at the same time the plasma current, vertical position, and some geometrical parameters. A general discussion on the design of plasma position, current, and shape controllers, including the choice of the controlled variables, can be found in [9].

The work described in this paper has been carried out in the framework of a project aimed at assessing the possibility of controlling accurately highly elongated plasmas at JET with the existing active circuits and control hardware [10]. One of the steps needed to achieve this objective has been the redesign of the JET shape controller, since the previous controller did not guarantee satisfying performance. This paper describes the features of the new JET controller, which has been called extreme shape controller (XSC). This new controller is the first example of a multivariable tokamak controller that enables to control with a high accuracy the overall plasma boundary, specified in terms of a certain number of gaps. The problem is formulated as an output regulation problem for a non-right-invertible plant, that is a plant that where the number of *independent* control variables is less than the number of *independent* outputs to regulate. In this case, it is not possible to guarantee that the difference between the reference and the controlled plant output (*tracking error*) is

zero at steady state. To tackle this problem, we essentially make use of a singular value decomposition in order to isolate the part of the plant output which can be better regulated at steady state. Moreover, the singular value decomposition gives us an insight into the steady-state control effort: since some of the singular values of the plant static gain are *small*, we truncate these singular values introducing a tradeoff between the tracking error and the control effort.

The activity that has been carried out and that is described in the paper is relevant in the perspective of International Thermonuclear Experimental Reactor (ITER). ITER is an international project aimed at demonstrating the scientific and technological feasibility of fusion energy [11]. The ITER tokamak is intended to provide the next major advancements in fusion physics and technology. Its design phase has been completed, and, in June, 2005, the representatives of the European Atomic Energy Community, of the Governments of the People's Republic of China, Japan, the Republic of Korea, the Russian Federation, and the United States of America have eventually agreed on building ITER (a 10bn-euro project) in France.

This paper is divided as follows. In Section II, we briefly describe the JET tokamak, then we discuss the control requirements and present the plant model that has been used for the design. In Section III, we present the technique we have adopted to design the controller. Section IV includes some experimental results. The conclusions are drawn in Section V.

II. Control Requirements and Simplified Plasma Modelling

A. JET Tokamak

JET is the world's largest fusion experiment. It was designed in the 1970s and started operation in 1983. A detailed description of JET and of the results over the first 20 years of research activity can be found in [12]. More recent results are reported in [13].

In the JET tokamak (see Figs. 2 and 4) there are eight poloidal field coils available to the plasma shape control system. These coils are denoted by P1,...,P4 (P-coils), and D1,...,D4 (D-coils). The P-coils are connected to form five circuits. The currents flowing in these circuits are indicated by I_{P1E}, I_{PFX}, I_{SHA}, I_{P4T}, I_{IMB}, whereas the currents flowing in the D-coils are indicated by $I_{\mathrm{D}i}$, with $i = 1, \ldots, 4$. Therefore, we have nine circuits available to the plasma control system. One of these circuits, P1E, is used to control the plasma current, whereas the other eight circuits can be used to control the plasma shape.

The controller we want to design should be able to control the plasma shape. One problem regarding the plasma shape control is the choice of the controlled variables. In this case, the plasma shape has been characterized by a finite number of parameters that are identified on the basis of the available magnetic measurements.

The plasma boundary in a poloidal cross section of a tokamak machine (see Fig. 3) is defined as the largest closed level line of the poloidal flux function which remains inside the vacuum chamber. For the cases we concentrate on, the plasma boundary does not touch the wall of the vacuum chamber; in this case, the poloidal flux function has a saddle in a point of the plasma boundary and in this point the level line is X-shaped, and therefore, this point is called X-point.

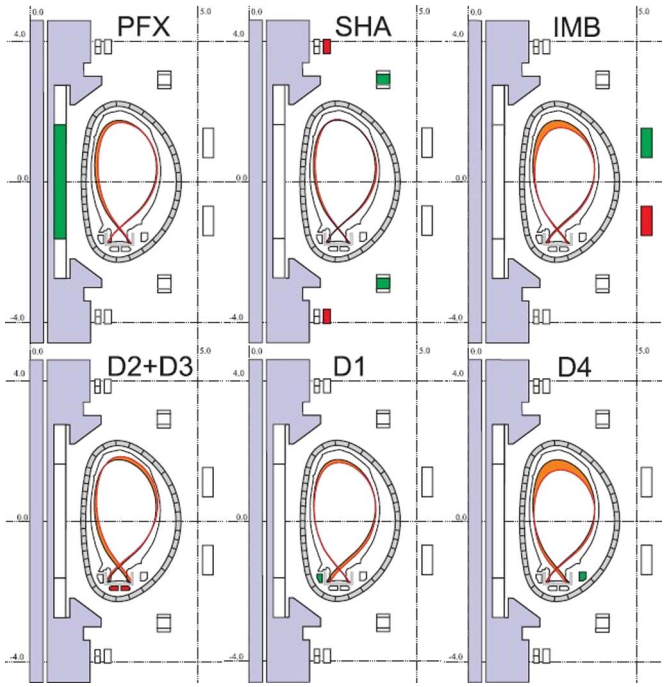

Fig. 4. Effect of the JET poloidal field currents on the shape. The orange band in the six plasma shape plots shows how a specific circuit current variation affects the plasma shape at steady state. The green and red colors used to highlight the various coils show the direction of the current variations relatively to the plasma current: the green color indicates the same direction and the red color the opposite direction. The figure clearly shows that current variations in different circuits cause similar variations on the shape; as a consequence, the *independent* degrees of freedom are less the total number of available poloidal field circuits.

For the case of the XSC, the controlled geometrical parameters controlled are a set of 28 gaps all around the vessel, the radial, and vertical position of the X-point, and finally, two parameters describing the strike point positions. The strike points are the contact points of the boundary with the tiles in the divertor zone (at the bottom in Fig. 3). Since the plasma exhaust is taken to the divertor, the tiles must be capable of handling high power flux (presently carbon-fiber composites). The strike points with these tiles still need to be carefully controlled.

To sum up, the system we want to control is characterized by the fact that the number of controlled outputs, equal to 32, is much larger than the number of control inputs, which is equal to 8.

B. Plant Model

A tokamak device is a system that includes the plasma, the active coils, and the metallic structures. It is a distributed parameter system whose dynamic behavior is described by a set of nonlinear PDEs, whereas most controller design techniques consider ODE models, usually linear and time-invariant. In this paper, we have made use of the LTI model described in [14] for the design and for the assessment of the controller performance through simulations, before the implementation on the plant.

JET plasmas are vertically unstable, mainly due to the D-shape of the plasma. The linearized model exhibit one real

positive eigenvalue with a *fast* growth time (1–10 ms). Therefore, a dedicated vertical stabilization system is needed [15].

In this paper, we focus on the design of the shape controller. As a consequence, we consider the model of the plasma already stabilized by the vertical stabilization controller. This model can be written in the standard state-space form

$$\frac{\mathrm{d}}{\mathrm{d}t}i = \mathcal{A}i + \mathcal{B}v \quad y = \mathcal{C}i$$

where i are the currents in the nine PF circuits and in the plasma, v are the voltages applied to the circuits, and y are the 32 controlled shape parameters. The plasma current is controlled using a dedicated single-input–single-output (SISO) loop, by means of a proportional controller which calculates the voltage to apply to the P1E circuit; the other eight circuits are used to control the plasma shape.

Tokamak reactors are pulsed machines; in each pulse the plasma is created, ramped up to the reference flat-top current, heated, maintained in a constant state, and finally, cooled down and terminated. More specifically, a plasma discharge can be roughly divided into the following four different phases.

1) *Breakdown*. During this phase, the plasma is formed: the hydrogen gas in the vacuum vessel is ionized. The conditions for the breakdown are in general difficult to achieve; usually some empirical "ecipes," depending on the plasma to form, are used.
2) *Ramp-Up*. During this phase, the plasma current, which is initially zero, reaches its desired steady-state value. Usually, the plasma current is linear or piecewise linear during this phase. Also, the other quantities that characterize the plasma reach their desired values.
3) *Flat-Top*. During this phase, all the quantities that characterize the plasma should remain as constant as possible. This is the most important, and long phase, during which the production of energy should happen. Therefore, the control requirements are very stringent. This is the phase we will focus on. Feedback control in this phase is very critical since the plasma current and shape need to be continuously adjusted and the disturbances that can happen must be rejected within a prescribed time.
4) *Ramp-Down*. The plasma current and all the other quantities are driven to zero. The plasma is extinguished.

At JET, the shape controller is separated in two parts: the inner loop (*current controller*) is dedicated to the control of the eight circuit currents, the outer loop (*shape controller*) calculates the currents that are needed to achieve and maintain a certain shape. This controller structure is motivated by the fact that there are some phases of a discharge, typically the ramp-up and ramp-down, when the control system is required to track some specified current waveforms, rather than guarantee a certain shape. In these cases, the outer loop is simply disconnected and the current reference directly goes to the current controller. Therefore, this separation in two loops can be seen as a requirement in the controller design, rather than a design choice.

The current controller, which is described in detail in [16], guarantees that the transfer matrix between the current references and the currents is approximately equal to the diagonal matrix $W(s) = (1/(1 + 0.1\ \mathrm{s}))I_8$, where I_8 is the 8×8 identity matrix. As a consequence, for the design of the plasma shape controller we are reduced to the following linearized simplified model:

$$Y(s) = P(s)U(s) \tag{1}$$

where $Y(s)$ are the controlled parameters described in Section II-A, $U(s)$ are the current references for the $m = 8$ circuits which are available to the shape controller, and

$$P(s) = \frac{C}{1 + s\tau} \tag{2}$$

with $\tau = 0.1$ s, and $C \in \mathbb{R}^{p\times m}$ with $p = 32$. The model (1) is the starting point for our controller design.

III. Controller Design

A. Requirements and Motivations

The main requirements for the shape control system that should be guaranteed are as follows.

- Once a certain desired shape for the plasma boundary is chosen by the physicists, it should be achieved by the feedback controller. In order to specify the required performance, the boundary is divided into five regions (see Fig. 3): the LOG region, the ROG region, the TOG region, the RIG region, and the divertor region. In certain regions, the precision is more critical (especially around ROG and the X-point), whereas in other regions a certain tolerance is acceptable (around 2–3 cm).
- The target shape should be maintained also in the presence of "disturbances" acting on the plasma. Typically, the amplitude of these disturbances is known in advance, and therefore, it is possible to evaluate in simulation the effects of the disturbances.
- The PF currents cannot exceed prescribed range of values; if this happens, the discharge is terminated by what is called a *soft stop*.

The benchmark for the new shape controller was given by the controller previously designed and in operation at JET. This controller [17] was simple in its structure, consisting of a static matrix gain, and guaranteed acceptable performance in most cases. Its main drawback is that it cannot guarantee a certain boundary shape but only control of very few gaps. There are some situations when control of these few gaps is not sufficient to guarantee the overall plasma shape requested by the physicists during the experiments. The challenge of the XSC was to guarantee a control as accurate as possible of the whole plasma shape with no modification to the existing active circuits and control hardware.

The shape control problem basically consists in determining the circuit currents that minimize the errors on the geometrical descriptors at steady state. Since we are using m currents, only m linear combinations of the geometrical descriptors can be reduced exactly to zero at steady state. Our problem then becomes that of determining the m linear combinations of the errors on the geometrical parameters that minimize the overall error in a

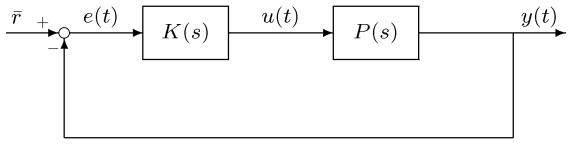

Fig. 5. Feedback scheme.

quadratic sense. On the other hand, once these m linear combinations have been selected, the m values of the control circuit currents at steady state are univocally determined. Hence, this approach could lead to high values of the currents; these values could possibly exceed the saturation limits. To overcome this problem, the number of linear combinations of geometrical descriptor errors to reduce to zero could be chosen to be less than m. This extra degree-of-freedom can be used to reduce the amplitude of the requested currents.

Remark 1: In JET, despite the availability of $m = 8$ separately powered poloidal circuits available for plasma shape control, there are in fact only five or six (depending on the magnetic configuration of the specific considered plasma) *independent* degrees of freedom (see Fig. 4).

In Section III-B, we show how the design problem can be tackled using a singular value decomposition approach. This approach can be cast in the more general framework of regulation for non-right-invertible plants, as shown in [18], [19], where a two-degree-of-freedom control scheme is considered.

B. Optimal Output Regulation

In our control problem, we want a constant reference $\bar{r}$ to be tracked by the controlled output variable $y(t)$. We will denote the tracking error by

$$e(t) := \bar{r} - y(t).$$

Let us consider a controller $K(s)$ with input $e(t)$ and output $u(t)$. Therefore, the closed-loop system is specified by the equations (see Fig. 5)

$$y = Pu \quad u = Ke \quad e = \bar{r} - y. \tag{3}$$

Our aim is to find a controller $K(s)$ that internally stabilizes the closed-loop system (3), and makes the error $e(t)$ *small* in some sense at steady state. When some conditions are verified [20], [21], it is possible to have $e(t) \to 0$ as $t \to +\infty$; then a possible choice is to minimize a weighted $\mathcal{L}_2$-norm of the error signal [22]. In our case, $p > m$ (number of output variables to regulate greater than number of control inputs), and the conditions that allow to have a zero steady-state error are typically not met. Therefore, we consider the problem of minimizing a steady-state performance index in the form

$$J = \lim_{t \to +\infty} e^T(t) Q e(t) \tag{4}$$

where $Q \in \mathbb{R}^{p \times p}$ is a positive definite weighting matrix.

Remark 2: In general, when considering the tracking problem the reference signal r is supposed to be generated by a so-called exosystem $\dot{r} = Sr$. In this paper, we limit our attention to constant references; otherwise, because of the fact that $p > m$, the optimal value of the cost function (4) could not be defined [that is the limit in (4) could not exist or could be unlimited].

Assuming that the controller $K(s)$ internally stabilizes the closed-loop system (3), it is possible to define the following quantities:

$$\bar{y} = \lim_{t \to +\infty} y(t) \quad \bar{u} = \lim_{t \to +\infty} u(t) \quad \bar{e} = \lim_{t \to +\infty} e(t)$$

where

$$\bar{e} = \bar{r} - \bar{y} = \bar{r} - C\bar{u}. \tag{5}$$

Remark 3: In deriving (5), we have exploited the fact that, provided that the closed-loop system (3) is internally stable, the relation

$$\bar{y} = C\bar{u} \tag{6}$$

holds also in the case when the plant matrix $P(s)$ is not asymptotically stable. When $P(s)$ is asymptotically stable, the C matrix is the static gain of $P(s)$.

Let us now consider the singular value decomposition of the following matrix:

$$\tilde{C} = Q^{1/2} C R^{-1/2} = U \Sigma V^T \tag{7}$$

where $\Sigma = \mathrm{diag}(\sigma_1, \sigma_2, \ldots, \sigma_m) \in \mathbb{R}^{m \times m}$, $U \in \mathbb{R}^{p \times m}$, $V \in \mathbb{R}^{m \times m}$, and $R \in \mathbb{R}^{m \times m}$ is a positive definite weighting matrix.

Remark 4: The two positive definite matrices R and Q are introduced to weight the steady-state control effort and tracking error, respectively. The way these matrices were chosen in the design of the controller for JET is discussed in Section IV.

In order to simplify the calculations that follow, in (7), we have considered the so-called economy size SVD [23]. We recall the following properties of the SVD (7):

$$V^T V = V V^T = I \tag{8a}$$

$$U^T U = I. \tag{8b}$$

The properties of the SVD imply that the columns of the matrix $Q^{-1/2} U \Sigma$ form a basis for the subspace of the obtainable steady-state output values. Now, we let $\bar{w} \in \mathbb{R}^m$ equal to

$$\bar{w} = \Sigma^{-1} U^T Q^{1/2} \bar{r}. \tag{9}$$

In this way, the reference signal can be split into two components, one of which lying in the subspace spanned by the matrix $Q^{-1/2} U \Sigma$; indeed we can write

$$\bar{r} = Q^{-1/2} U \Sigma \bar{w} + \bar{b}. \tag{10}$$

From (10) and (9), making use of (8b), it follows that $\bar{b}$ satisfies

$$U^T Q^{1/2} \bar{b} = 0. \tag{11}$$

Now let us decompose the plant output accordingly to what has been done for the reference [see (9)]. Therefore, let us define

$$z(t) = \Sigma^{-1} U^T Q^{1/2} y(t). \tag{12}$$

The signal $z(t)$ represents the component of the output signal $y(t)$ that can be actually regulated; it has the same dimension of $u(t)$.

Denoting by $\bar{z}$ the steady-state value of $z(t)$, we have

$$\begin{aligned} \bar{z} &= \Sigma^{-1} U^T Q^{1/2} \bar{y} = \Sigma^{-1} U^T Q^{1/2} C \bar{u} \\ &= \Sigma^{-1} U^T U \Sigma V^T R^{1/2} \bar{u} = V^T R^{1/2} \bar{u} \end{aligned} \tag{13}$$

where we have used (6), (7), and (8b). From (13), using (8a), we obtain

$$\bar{u} = R^{-1/2} V \bar{z}. \tag{14}$$

Finally, using (6), we have

$$\bar{y} = C\bar{u} = Q^{-1/2} U \Sigma V^T R^{1/2} \bar{u} = Q^{-1/2} U \Sigma \bar{z}. \tag{15}$$

The decomposition (10) has a direct consequence on the cost function (4); indeed using (10) and (15) it is possible to write

$$\bar{e} = \bar{r} - \bar{y} = Q^{-1/2} U \Sigma \bar{w} + \bar{b} - Q^{-1/2} U \Sigma \bar{z}.$$

In this way, using (11), we obtain

$$\begin{aligned} J &= (\bar{w} - \bar{z})^T \Sigma^2 (\bar{w} - \bar{z}) + \bar{b}^T Q \bar{b} \\ &= \sum_{i=1}^{m} \sigma_i^2 (\bar{w}^i - \bar{z}^i)^2 + \bar{b}^T Q \bar{b} \end{aligned} \tag{16}$$

where $\bar{w}^i$ (respectively, $\bar{z}^i$) indicate the components of $\bar{w}$ (respectively, $\bar{z}$).

Remark 5: The reason for our choice (9) is that we need property (11) to rewrite the performance index (4) as in (16). Moreover, note that in the case $Q = I$, with the choice (9), the vectors $Q^{-1/2} U \Sigma \bar{w}$ and $\bar{b}$ are orthogonal.

The quadratic term involving the vector $\bar{b}$ in (16) does not depend on the choice of the controller, but only on the reference signal $\bar{r}$ to be tracked. Therefore, minimizing J is equivalent to minimizing the cost function

$$\tilde{J} = (\bar{w} - \bar{z})^T \Sigma^2 (\bar{w} - \bar{z}) = \sum_{i=1}^{m} \sigma_i^2 (\bar{w}^i - \bar{z}^i)^2. \tag{17}$$

Let us imagine for the moment that we are able to design a controller such that the index (17) be zero. In this case, we would have that

$$\lim_{t \to +\infty} (\bar{w} - z(t)) = \bar{w} - \bar{z} = 0. \tag{18}$$

Making use of (14), (18), and (9), we can calculate the control effort $\bar{u}$ that we would need at steady state. It would evaluate to

$$\bar{u} = R^{-1/2} V \bar{z} = R^{-1/2} V \bar{w} = R^{-1/2} V \Sigma^{-1} U^T Q^{1/2} \bar{r}.$$

Therefore, the steady-state control effort is related to the smallest singular value σ_m of $\tilde{C}$ [see (7)] since

$$\max_{\|Q^{1/2}\bar{r}\|=1} \|R^{1/2}\bar{u}\| = \|V \Sigma^{-1} U^T\| = \frac{1}{\sigma_m}. \tag{19}$$

Remark 6: It is interesting to note that, once an R matrix has been fixed, the steady-state value $\bar{u}$ does not depend on the controller parameters, provided that the index (17) be zero. This is a consequence of the fact that we drive to zero a number m of error linear combinations, which is equal to the number of control inputs, and this can be done in an unique way.

Equation (19) shows that if we minimize the cost function (17), this can turn out in unacceptable steady-state values of $u(t)$. This is indeed true in our case for the JET tokamak, where an analysis of the singular values showed that $\sigma_1 > \cdots > \sigma_k \gg \sigma_{k+1} > \cdots > \sigma_m$ for $k = 5$ (see also Remark 1). As a consequence [see (16) and (19)], if we minimize (17) taking into account all of the singular values, we spend a lot of control effort gaining just a little improvement in the value of the cost function. This suggests that we modify the cost function (17) neglecting the terms corresponding to the singular values σ_i with $i > k$ (the smallest ones). In this way, we are using just k linear combinations of the inputs and, therefore, we can minimize a weighted norm of the steady-state control vector $\bar{u}$, since this steady-state value is no more independent of the controller parameters (see Remark 6). To this aim, we consider the new cost function (with $k < m$ terms)

$$\tilde{J}_1 = \sum_{i=1}^{k} \sigma_i^2 (\bar{w}^i - \bar{z}^i)^2. \tag{20}$$

Hence, our aim becomes to find a controller structure that solves the following *optimization problem*:

$$\boxed{\min_{\bar{u}} \bar{u}^T R \bar{u} \quad \text{such that } \tilde{J}_1 = 0.} \tag{21}$$

Let us introduce the following partitions:

$$U = (U_1 \quad U_2), \quad V = (V_1 \quad V_2), \quad \Sigma = \begin{pmatrix} \Sigma_1 & 0 \\ 0 & \Sigma_2 \end{pmatrix}$$

$$z(t) = \begin{pmatrix} z_a(t) \\ z_b(t) \end{pmatrix}, \quad \bar{z} = \begin{pmatrix} \bar{z}_a \\ \bar{z}_b \end{pmatrix}, \quad \bar{w} = \begin{pmatrix} \bar{w}_a \\ \bar{w}_b \end{pmatrix}$$

where $U_1 \in \mathbb{R}^{p\times k}$, $V_1 \in \mathbb{R}^{m\times k}$, $\Sigma_1 \in \mathbb{R}^{k\times k}$, $z_a(t) \in \mathbb{R}^k$, $\bar{z}_a \in \mathbb{R}^k$, and $\bar{w}_a \in \mathbb{R}^k$. Using these partitions, (8) becomes

$$\begin{pmatrix} V_1^TV_1 & V_1^TV_2 \\ V_2^TV_1 & V_2^TV_2 \end{pmatrix} = \begin{pmatrix} I & 0 \\ 0 & I \end{pmatrix} \tag{22a}$$

$$V_1V_1^T + V_2V_2^T = I \tag{22b}$$

$$\begin{pmatrix} U_1^TU_1 & U_1^TU_2 \\ U_2^TU_1 & U_2^TU_2 \end{pmatrix} = \begin{pmatrix} I & 0 \\ 0 & I \end{pmatrix}. \tag{22c}$$

Our performance index (20) can be rewritten as

$$\tilde{J}_1 = (\bar{w}_a - \bar{z}_a)^T\Sigma_1^2(\bar{w}_a - \bar{z}_a). \tag{23}$$

From (9), we have that

$$\bar{w}_a = \Sigma_1^{-1}U_1^TQ^{1/2}\bar{r} \tag{24}$$

whereas, from (12), we have

$$z_a(t) = \Sigma_1^{-1}U_1^TQ^{1/2}y(t). \tag{25}$$

Finally, making use of (6), (7), and (22c), we have

$$\begin{aligned} \bar{z}_a &= \Sigma_1^{-1}U_1^TQ^{1/2}\bar{y} \\ &= \Sigma_1^{-1}U_1^TQ^{1/2}Q^{-1/2}U\Sigma V^TR^{1/2}\bar{u} \\ &= V_1^TR^{1/2}\bar{u}. \end{aligned} \tag{26}$$

We cannot directly obtain $\bar{u}$ from (26), unless we let

$$u(t) = R^{-1/2}V_1u_1(t). \tag{27}$$

In this way

$$\bar{u} = R^{-1/2}V_1\bar{u}_1$$

and substitution in (26), recalling that $V_1^TV_1 = I$ [see (22a)], gives

$$\bar{z}_a = \bar{u}_1.$$

Therefore, we have

$$\bar{u} = R^{-1/2}V_1\bar{z}_a. \tag{28}$$

Now, accordingly to the choice (27), and in order to reduce our design to a square $k \times k$ controller, let

$$K(s) = R^{-1/2}V_1\tilde{K}(s)\Sigma_1^{-1}U_1^TQ^{1/2}. \tag{29}$$

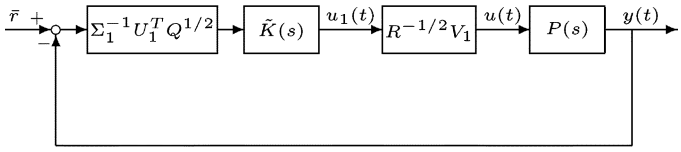

Fig. 6. Feedback scheme with the controller (29).

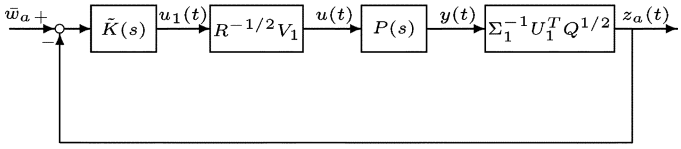

Fig. 7. Feedback scheme equivalent to the one in Fig. 6.

In this way, we arrive to the feedback scheme of Fig. 6.

Since we want to track constant references with as small as possible error, we include an integral action in $\tilde{K}(s)$, letting

$$\tilde{K}(s) = \tilde{K}_a(s) + \frac{\tilde{K}_b(s)}{s} \tag{30}$$

so that (29) becomes

$$K(s) = R^{-1/2}V_1\left(\tilde{K}_a(s) + \frac{\tilde{K}_b(s)}{s}\right)\Sigma_1^{-1}U_1^TQ^{1/2}. \tag{31}$$

Using (24) and (25), it is easy to show that the feedback scheme of Fig. 6 is equivalent to the one shown in Fig. 7; hence, provided that the closed-loop system is internally stable, the integral action in the controller (30) guarantees that

$$\lim_{t\to+\infty}(\bar{w}_a - z_a(t)) = \bar{w}_a - \bar{z}_a = 0 \tag{32}$$

and, therefore, the performance index $\tilde{J}_1$ defined in (23) is equal to zero.

Now we can prove the following result.

Theorem 1: Any controller with the structure (31), provided that it internally stabilizes the closed-loop system (3), solves the optimization problem (21).

Proof: The optimization problem (21) consists in finding the minimum of $\bar{u}^TR\bar{u}$ with the constraint that $\tilde{J}_1 = 0$. First note that [see (23)] requiring that $\tilde{J}_1$ be zero implies that

$$\bar{w}_a = \bar{z}_a.$$

Then, as a consequence of (26), we have that

$$\bar{w}_a = V_1^TR^{1/2}\bar{u}.$$

Therefore, our minimization problem can be rewritten as

$$\min_{\bar{u}} \bar{u}^TR\bar{u} \quad \text{such that } \bar{w}_a = V_1^TR^{1/2}\bar{u}.$$

It is easy to show by standard static optimization techniques that this minimum value is attained when

$$\bar{u} = R^{-1/2} V_1 \bar{w}_a. \tag{33}$$

On the other hand, using the controller structure (31) the performance index $\tilde{J}_1$ is zero and [see (28)]

$$\bar{u} = R^{-1/2} V_1 \bar{z}_a.$$

The fact that $\bar{z}_a = \bar{w}_a$ [see (32)] completes the proof. ■

Remark 7: From (33) and (24), we have that the minimum value of $\bar{u}$ is given by

$$\bar{u} = R^{-1/2} V_1 \bar{w}_a = R^{-1/2} V_1 \Sigma_1^{-1} U_1^T Q^{1/2} \bar{r}.$$

C. Design of PI Controllers

Theorem 1 guarantees that any controller with the structure (31) solves the optimization problem (21), provided that it is an internally stabilizing controller. Therefore, our last step is the design of a stabilizing controller with the specified structure.

Let us choose $\tilde{K}(s)$ [see (30)] in the simplified form

$$\tilde{K}(s) = K_P + \frac{K_I}{s}$$

with K_P, $K_I \in \mathbb{R}^{k \times k}$. In order to find a convenient choice for K_P and K_I, let us evaluate the loop gain transfer matrix $F(s)$; recalling (1) and (7), and using (22a) and (22c), we have

$$\begin{aligned} F(s) &= \Sigma_1^{-1} U_1^T Q^{1/2} P(s) R^{-1/2} V_1 \tilde{K}(s) \\ &= \Sigma_1^{-1} U_1^T Q^{1/2} \frac{Q^{-1/2} U \Sigma V^T R^{1/2}}{1 + s\tau} R^{-1/2} V_1 \tilde{K}(s) \\ &= \Sigma_1^{-1} (I \quad 0) \begin{pmatrix} \Sigma_1 & 0 \\ 0 & \Sigma_2 \end{pmatrix} \begin{pmatrix} I \\ 0 \end{pmatrix} \frac{\tilde{K}(s)}{1 + s\tau} \\ &= \frac{\tilde{K}(s)}{1 + s\tau}. \end{aligned}$$

Therefore, exploiting the properties of the singular value decomposition, if we choose K_P and K_I as diagonal matrices

$$K_P = \operatorname{diag}(K_{P_1}, \ldots, K_{P_k}) \quad K_I = \operatorname{diag}(K_{I_1}, \ldots, K_{I_k})$$

we reduce our problem to k decoupled SISO problems (see Fig. 8). Since we are controlling k linear combinations of the output $y(t)$, the most reasonable choice is to let

$$K_P = k_p I \quad K_I = k_i I.$$

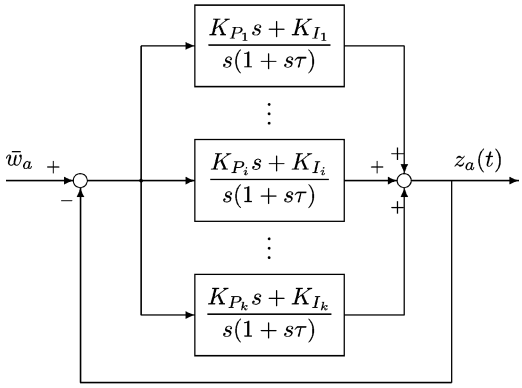

Fig. 8. Decoupled scheme for the PI design.

The values of the two scalars k_p and k_i have been chosen so as to assign to each SISO loop the behavior of a second-order system with a natural frequency of 25 rad/s and a damping factor of 0.7.

IV. Experimental Results

The XSC has been implemented at JET on a 400 MHz G4 PowerPC. The controller software architecture has been designed so that it allows to test all the software offline, since at JET long commissioning periods are not available (see [24] for details).

The XSC has been designed to control the plasma shape during the flat-top phase, when the plasma current has a constant magnitude; as a matter of fact it has been used at JET also during large excursions of the plasma current: maintaining the plasma shape constant during such large excursions is very demanding, since all the plasma parameters are changing and the assumption that a single linearized model can describe the plasma behavior is no longer valid.

As already specified in Section III-A, during the discharges at JET, there are some regions of the plasma boundary that need to be controlled more accurately; this is the case for instance (see Fig. 3) of the region around the ROG gap, or of the gaps in the divertor region: therefore, the gaps belonging to these regions have been assigned a higher weight in the Q matrix. On the other hand, the elements of the R matrix have been chosen depending on the saturation values of the different circuits: the higher the "room" for the feedback control, the lower the element of the R matrix.

Hereafter, we show the results obtained during the JET shot number 62837, where the XSC took control during the plasma flat-top at $t = 54$ s. The controller was asked to track two different shapes: one at $t = 54$ s (Test 1) and the second one at $t = 61$ s (Test 2).

Let us denote by $\bar{r}$ the desired constant reference; by t_{s} the switching time, that is the time when the reference on the shape is changed; by $t_{\mathrm{tr}} = 3$ s a so-called *transition time*; by y the shape geometrical variables to regulate. Then, to avoid large

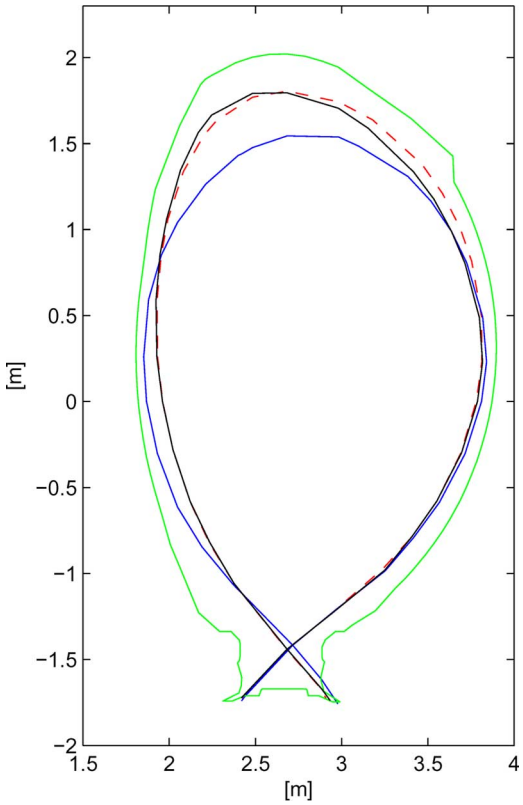

Fig. 9. Test 1 of the XSC during the shot #62837: the switching time is $t_{\rm s} = 54$ s and the transition time $t_{\rm tr} = 3$ s. The figure shows: 1) the reference shape to be tracked (dashed in red); 2) the plasma boundary at $t = 54$ s (solid in blue); 3) the plasma boundary at $t = 57$ s (solid in black). The vessel is shown in green.

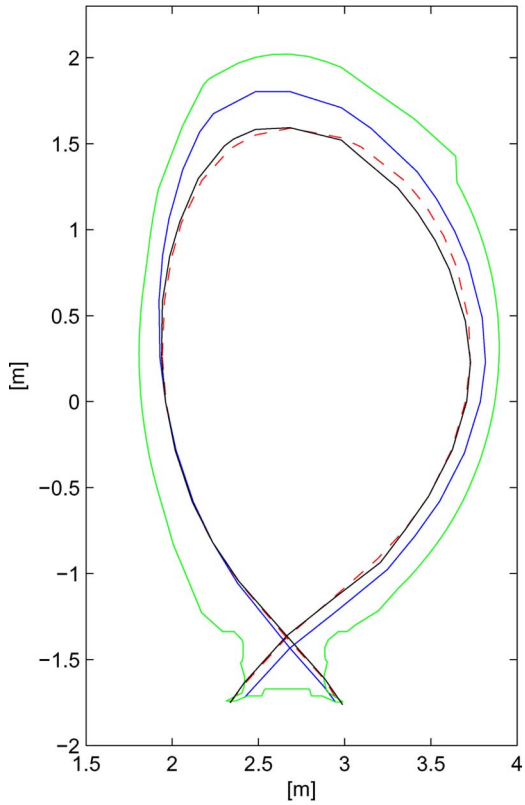

Fig. 10. Test 2 of the XSC during the shot #62837: the switching time is $t_{\rm s} = 61$ s and the transition time $t_{\rm tr} = 3$ s. The Figure shows: 1) the reference shape to be tracked (dashed in red); 2) the plasma boundary at $t = 61$ s (solid in blue); 3) the plasma boundary at $t = 64$ s (solid in black). The vessel is shown in green.

control signals, the shape reference given to the controller is linearly interpolated over $t_{\rm tr} = 3$ s in the following way:

$$r(t) = \begin{cases} y(t_{\rm s}) + (\bar{r} - y(t_{\rm s}))\,\frac{t-t_{\rm s}}{t_{\rm tr}}, & t_{\rm s} \le t \le t_{\rm s} + t_{\rm tr} \\ \bar{r}, & t > t_{\rm s} + t_{\rm tr}. \end{cases}$$

Figs. 9 and 10 show the reference shape and the shape that has been obtained with the XSC for Test 1 and 2 cases, respectively: in both cases the shape is reached with a small steady-state error. Fig. 11 shows the average value of the error on the 32 controlled gaps, evaluated as

$$e(t) = \begin{cases} \frac{||\bar{r}_1 - y(t)||_1}{32}, & 54 \le t \le 61 \\ \frac{||\bar{r}_2 - y(t)||_1}{32}, & t > 61 \end{cases}$$

where $\bar{r}_1$ and $\bar{r}_2$ denote the first (Test 1) and the second (Test 2) constant reference shapes, respectively. As it can be seen, initially, when the XSC is switched on, at $t = 54$ s the mean error is of about 8 cm, then the XSC reduces this error to less than 2 cm in about 3 s (the transition time interval); a similar behavior can be observed at $t = 61$ s, when the shape reference is changed. Fig. 12 shows the tracking results for the two gaps ROG and TOG, and for the radial and vertical position of the X-point (see Fig. 4).

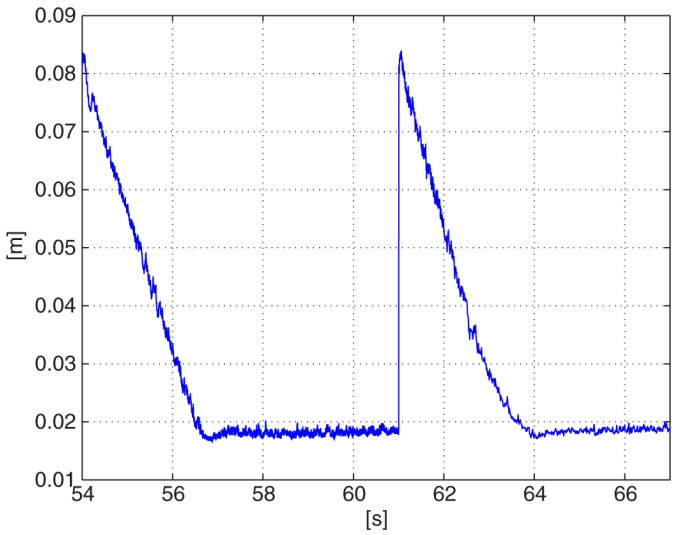

Fig. 11. Experimental test of the XSC during the shot #62837: the average error on the 32 controlled shape variables when using the XSC.

The XSC has been successfully used also in the presence of injection of heating power to the plasma. These injections act as disturbances for the shape, which, without adequate feedback control, would modify. The XSC has been able to counteract these disturbances, rejecting them, and keeping the shape almost unmodified.

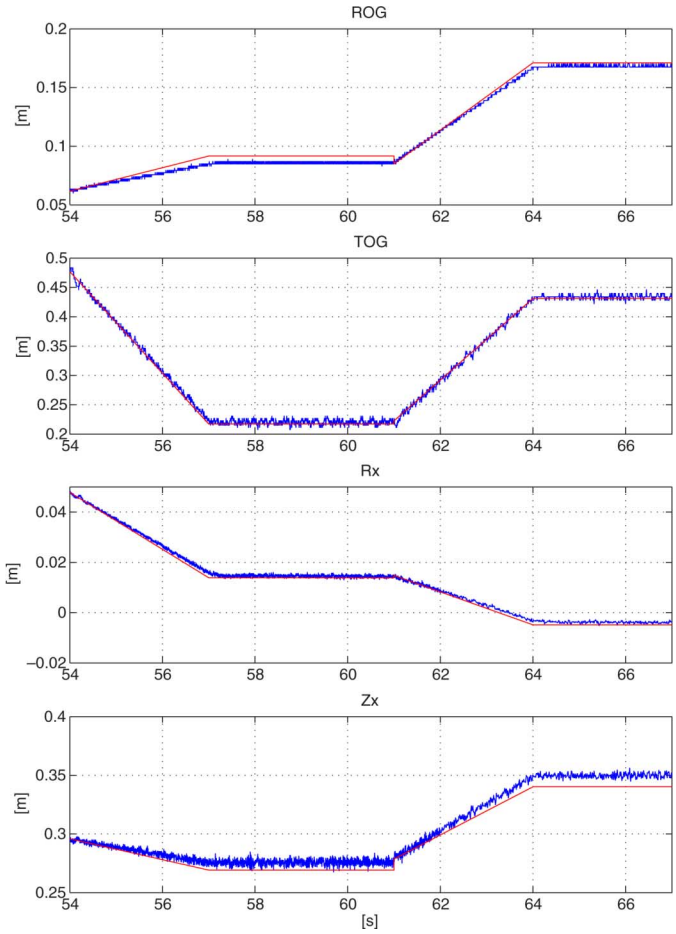

Fig. 12. Experimental test of the XSC during the shot #62837: the behavior of two gaps and of the X-point while using the XSC. From the top to the bottom: ROG, TOG, the radial and the vertical position of the X-point. The experimental traces are shown in blue, the references are shown in red.

V. Conclusion

In this paper, we have described the XSC which has been recently designed and implemented on the JET tokamak. This new controller gives the possibility of controlling the plasma shape, specified in terms of some plasma-wall distances, and of maintaining it even in the presence of significant variations of critical plasma parameters.

The design procedure is essentially based on the singular value decomposition of the plant output matrix. This procedure allows us to take into account all the different requirements, specified in terms of accuracy on the controlled variables and of maximum allowable control effort.

The new controller has been fully commissioned on the JET tokamak. It is now used during the experiments where accurate control of the plasma shape is needed.

References

[1] P. Vyas, A. W. Morris, and D. Mustafa, "Vertical position control on COMPASS-D," *Fusion Technol.*, vol. 33, no. 2, pp. 97–105, Mar. 1998.

[2] J. R. Gossner, P. Vyas, B. Kouvaritakis, and A. W. Morris, "Application of cautious stable predictive control to vertical positioning in COMPASS-D Tokamak," *IEEE Trans. Control Syst. Technol.*, vol. 7, no. 5, pp. 580–587, Sep. 1999.

[3] L. Scibile and B. Kouvaritakis, "A discrete adaptive near-time optimum control for the plasma vertical position in a Tokamak," *IEEE Trans. Control Syst. Technol.*, vol. 9, no. 1, pp. 148–162, Jan. 2001.

[4] E. Schuster, M. L. Walker, D. A. Humphreys, and M. Krstić, "Plasma vertical stabilization with actuation constraints in the DIII-D tokamak," *Automatica*, vol. 41, pp. 1173–1179, 2005.

[5] J. E. Morelli, A. Hirose, and H. C. Wood, "Fuzzy-logic-based plasma-position controller for STOR-M," *IEEE Trans. Control Syst. Technol.*, vol. 13, no. 2, pp. 328–337, Mar. 2005.

[6] M. L. Walker, D. A. Humphreys, J. A. Leuer, and J. R. Ferron, "Development of multivariable control techniques for use with the DIII-D plasma control system," General Atomics, Fusion Technology, Tech. Rep. GA-A23151, Jun. 1999.

[7] M. Ariola, G. Ambrosino, J. B. Lister, A. Pironti, F. Villone, and P. Vyas, "A modern plasma controller tested on the TCV tokamak," *Fusion Technol.*, vol. 36, no. 2, pp. 126–138, Sep. 1999.

[8] M. Ariola, G. Ambrosino, A. Pironti, J. B. Lister, and P. Vyas, "Design and experimental testing of a robust multivariable controller on a tokamak," *IEEE Trans. Control Syst. Technol.*, vol. 9, no. 6, pp. 831–838, Nov. 2001.

[9] M. Ariola, A. Pironti, and A. Portone, "A framework for the design of a plasma current and shape controller in next-generation tokamaks," *Fusion Technol.*, vol. 36, no. 3, pp. 263–277, Nov. 1999.

[10] F. Crisanti *et al.*, "Upgrade of the present JET shape and vertical stability controller," *Fusion Eng. Des.*, vol. 66–68, pp. 803–807, Sep. 2003.

[11] C. C. Baker, B. Montgomery, and K. L. Wilson, "ITER—A world class challenge and opportunity," *IEEE Trans. Appl. Supercond.*, vol. 5, no. 2, pp. 61–68, Jun. 1995.

[12] J. Wesson, *The Science of JET*. Abingdon, Oxon: JET Joint Undertaking, Mar. 2000 [Online]. Available: http://www.jet.efda.org/documents/wesson/wesson.html

[13] J. Pamela *et al.*, "Overview of JET results," *Nuclear Fusion*, vol. 42, no. 12, pp. 1540–1554, Dec. 2003.

[14] R. Albanese, G. Calabrò, M. Mattei, and F. Villone, "Plasma response models for current, shape and position control in JET," *Fusion Eng. Des.*, vol. 66–68, pp. 715–718, Sep. 2003.

[15] F. Sartori, G. De Tommasi, and F. Piccolo, "The Joint European Torus," *IEEE Control Syst. Mag.*, vol. 26, no. 2, pp. 64–78, Apr. 2006.

[16] M. Ariola and A. Pironti, "Plasma shape control for the JET tokamak," *IEEE Control Syst. Mag.*, vol. 25, no. 5, pp. 65–75, Oct. 2005.

[17] M. Garibba, R. Litunovsky, P. Noll, and S. Puppin, "The new control scheme for the JET plasma position and current control system," in *Proc. 15th SOFE Conf.*, Lisbon, 1996, pp. 33–36.

[18] G. Ambrosino, M. Ariola, and A. Pironti, "Optimal regulation for linear non right-invertible plants," in *Proc. 42nd IEEE Conf. Dec. Control*, Dec. 2003, pp. 869–873.

[19] G. Ambrosino, M. Ariola, and A. Pironti, "Optimal steady-state control for linear non right-invertible systems," *IET Control Theory Appl.*, vol. 1, no. 3, pp. 604–610, May 2007.

[20] E. J. Davison, "A generalization of the output control of linear multivariable systems with unmeasurable arbitrary disturbances," *IEEE Trans. Autom. Control*, vol. 20, no. 6, pp. 788–792, Dec. 1975.

[21] B. A. Francis, "The linear multivariable regulator problem," *SIAM J. Control Opt.*, vol. 15, no. 3, pp. 486–505, 1977.

[22] A. Saberi, A. Stoorvogel, P. Sannuti, and G. Shi, "On optimal output regulation for linear systems," *Int. J. Control*, vol. 76, no. 4, pp. 319–333, 2003.

[23] G. Golub and C. F. Van Loan, *Matrix Computations*, 3rd ed. Baltimore, MD: Johns Hopkins Univ. Press, 1996.

[24] G. De Tommasi, F. Piccolo, A. Pironti, and F. Sartori, "A flexible software for real-time control in nuclear fusion experiments," *Control Eng. Practice*, vol. 14, no. 11, pp. 1387–1393, 2006.

Giuseppe Ambrosino received the magna cum laude degree in electronic engineering from the Università di Napoli, Napoli, Italy, in 1975.

From 1977 to 1978, he studied and researched at Politecnico di Milano, Milano, Italy. From 1979 to 1986, he was an Associate Professor with the Department of System Theory and Automatic Control, Università di Napoli. Since 1986, he has been a Full Professor of automatic control. His current research interests include applications of control theory in many fields, such as aerospace, thermonuclear plasmas, and industrial automation. He has been involved in several international projects in the field of fusion such as NET, Ignitor, ITER, FTU, and JET.

Marco Ariola (SM'06) was born in Naples, Italy, in 1971. He received the Laurea degree in electronic engineering (cum laude) and the Research Doctorate degree in electronic engineering and computer science from the University of Naples Federico II, Naples, Italy, in 1995 and 2000, respectively.

Currently, he is an Associate Professor with the Technology Department, University of Naples Parthenope. From September 1998 to February 1999, he was a Visiting Scholar with the Department of Electrical and Computer Engineering, University of New Mexico, Albuquerque. His research interests include statistical control, robust control, control of nuclear fusion devices, control of aerospace systems. He has published more than 100 journal papers, conference papers, articles in books and encyclopedias.

Prof. Ariola has been member of the International Program Committee of the 42nd IEEE Conference on Decision and Control held in December 2003. He has served as an Associate Editor of the IEEE Control System Society Conference Editorial Board since 2006.

Alfredo Pironti received the Laurea degree (cum laude) in electronic engineering and the Ph.D. degree in electronic and computing engineering from the University of Naples Federico II, Naples, Italy, in 1991 and 1995, respectively.

Since 1991, he has been with the Dipartimento di Informatica e Sistemistica, University of Naples, where he is currently an Associate Professor of system theory. He has been a Visiting Researcher with the Max Planck Institute for Plasma Physics, Garching, Germany, the Center for Control Engineering and Computation, University of California at Santa Barbara, and at the ITER Joint Work Site, Naka, Japan. His research interests include robust control of uncertain systems and the application of feedback control to nuclear fusion problems.

Filippo Sartori received the Laurea Degree (cum laude) in electronic engineering from the University of Padua, Padua, Italy, in 1991, and the Ph.D. degree in electrical engineering from the University of Naples, Naples, Italy, in 2004.

In 1999, he joined JET, where he is currently responsible for the magnetic plasma control systems. In 1993, he joined JET as a student to participate to the development of the digital plasma shape control systems. In 1997, he joined RFX Padua and, in 1998, he returned to the U.K. to work on embedded control of synchronous motors for the electric automotive industry.